Periodico di Mineralogia (2011), 80, 3 (Spec. Issue), 407-432 DOI: 10.2451/2011PM0028

PERIODICO di MINERALOGIA
established in 1930

An International Journal of
MINERALOGY, CRYSTALLOGRAPHY, GEOCHEMISTRY,
ORE DEPOSITS, PETROLOGY, VOLCANOLOGY
and applied topics on *Environment*, *Archeometry* and *Cultural Heritage*

Karst bauxites in the Campania Apennines (southern Italy): a new approach

Nicola Mondillo[1,*], Giuseppina Balassone[1], Maria Boni[1] and Gavyn Rollinson[2]

[1] Dipartimento Scienze della Terra, Università degli Studi di Napoli Federico II,
Via Mezzocannone 8, 80134 Napoli, Italy
[2] Camborne School of Mines, University of Exeter, Cornwall Campus, Penryn, Cornwall TR10 9EZ,
United Kingdom
* Corresponding author: *nicola.mondillo@unina.it*

Abstract

In this study new data on two bauxite districts in the Campania region (southern Italy) are reported: the Matese Mts. and the Caserta province, exploited in the first part of the XX century. The nature and distribution of diagenetic and detrital mineral phases were investigated by means of transmitted-light and scanning electron (SEM) microscopy, X-ray powder diffraction (XRPD) and energy dispersive spectroscopic microanalysis (EDS), whole-rock geochemical analyses (ICP-OES and ICP-MS), complemented by preliminary QEMSCAN® investigation. The textures of the bauxite ore range between oolitic and oolitic-conglomeratic and arenitic. Boehmite is the most abundant phase, while other Al-bearing phases (gibbsite and diaspore) are very subordinate. The Fe-minerals hematite, goethite and lepidocrocite occur, and Ti-minerals anatase and rutile are ubiquitous. Among clay minerals, kaolinite is prevailing at the Regia Piana (Matese Mts.) and illite-montmorillonite in the Caserta province. Most recorded trace minerals are quartz, calcite, zircon and monazite. Small clusters of not previously detected qandilite [$(Mg, Fe^{2+})_2(Ti, Fe^{3+}, Al)\ O_4$], and of hercynite-type spinels also occur. By means of QEMSCAN® it has been possible to better recognize some diagenetic textures (e.g. mainly matrix- or ooids-supported bauxite, the clay/Al-hydroxides distribution etc.) and to detect other detrital minerals (feldspar, muscovite, olivine, titanite and possibly a serpentine/talc-like phase). A similar detrital mineral association has been found also in the Aptian "*Orbitoline*" marls, which are marine sediments supposed to be the non-weathered equivalent of bauxites.

Very detailed data about major, minor and trace element (comprising "*bauxitophile*" and REEs) concentrations and some significant geochemical ratios are reported for the bauxite samples, and a new interpretation on the possible source of the parent material has been proposed. The detrital heavy mineral association may suggest not only a windblown volcanic source material (Dinarides explosive volcanism?), as hypothesized in literature, but also a

partial origin from an exposed terrain. The exact nature and paleogeographic position of this source could not be determined by chemical analyses of major and trace elements (including REE), Eu/Eu* and TiO_2/Al_2O_3 ratios and Ni-Cr contents. However, due to the isolated position of the Appennine carbonate platform during the Cretaceous, the paleogeographic model precludes any possible fluviomarine transport for the source material (windblown?) of the bauxites.

Key words: bauxite; southern Italy; Campania region; mineralogy and petrography; geochemistry; genetic model.

Introduction

Bauxites are economic concentrations of aluminum, developed from the weathering of alumosilicate-rich parent rocks. These residual deposits are mainly formed under humid tropical to sub-tropical climates, with rainfalls in excess of 1.2 m and annual mean temperatures higher than 22 °C (Bárdossy and Aleva, 1990). Aluminum in bauxites is known to be precipitated in the form of gibbsite [$Al(OH)_3$] or amorphous Al-hydroxides. Metabauxites (bauxites subjected to several diagenetic stages) consist mainly of boehmite [AlO(OH)], which is less hydrated than gibbsite, and diaspore. Iron is separated from aluminum and is frequently concentrated as hematite >> goethite.

Though several intense palaeoweathering periods have been recorded in the European continent from Upper Paleozoic to Mesozoic, the Cretaceous-Eocene interval is considered the most favorable for bauxitization. In Europe, the Cretaceous marked one distinctive period of closure of part of the Tethys Ocean accompanied by collision, uplift, and exhumation of both ophiolitic suites and sedimentary successions. Many of the circum-Mediterranean bauxites, including those located in the Italian peninsula are Cretaceous in age, all formed in karstic environments (*karst bauxites*) of exhumed carbonates, which behaved as both a physical and chemical trap. The karstic network provided optimum drainage, necessary for further desilicification of bauxites, as well as providing a protected environment from later surface erosion (Bárdossy, 1982).

Most European bauxites are characterized by minerals deposited in high Eh environments, and rich in "*bauxitophile*" trace elements, like V, Co, Ni, Cr, Zr and locally in REEs (Bárdossy, 1982).

Bauxite deposits, at present uneconomic due to their small dimensions and scattered distribution, occur along a Cretaceous stratigraphic gap in the Mesozoic carbonate platforms of Central and Southern Italy (Figure 1): in the Abruzzi-Molise, Campania and in Apulia districts. The main horizons are Aptian to Turonian in age and prevailingly boehmitic (Bárdossy et al., 1977). Despite their low economic value, the bauxites of Southern Apennines can be considered as a model analogue for other, far more economic karst bauxite deposits in the world.

The data presented here refer to two small districts in Campania, where bauxites were exploited in the first part of the 20th century: the Matese Mts. and the Caserta province. By means of transmitted-light and scanning electron (SEM) microscopy, X-ray powder diffraction (XRPD) and energy dispersive spectroscopic microanalysis (EDS) mineralogy, and whole-rock geochemical analyses, complemented by preliminary QEMSCAN® investigation, this study documents the distribution of diagenetic and detrital mineral phases, and draws a renewed mineralogical and genetic picture for the Campania bauxites, to be compared to other occurrences in the Mediterranean region.

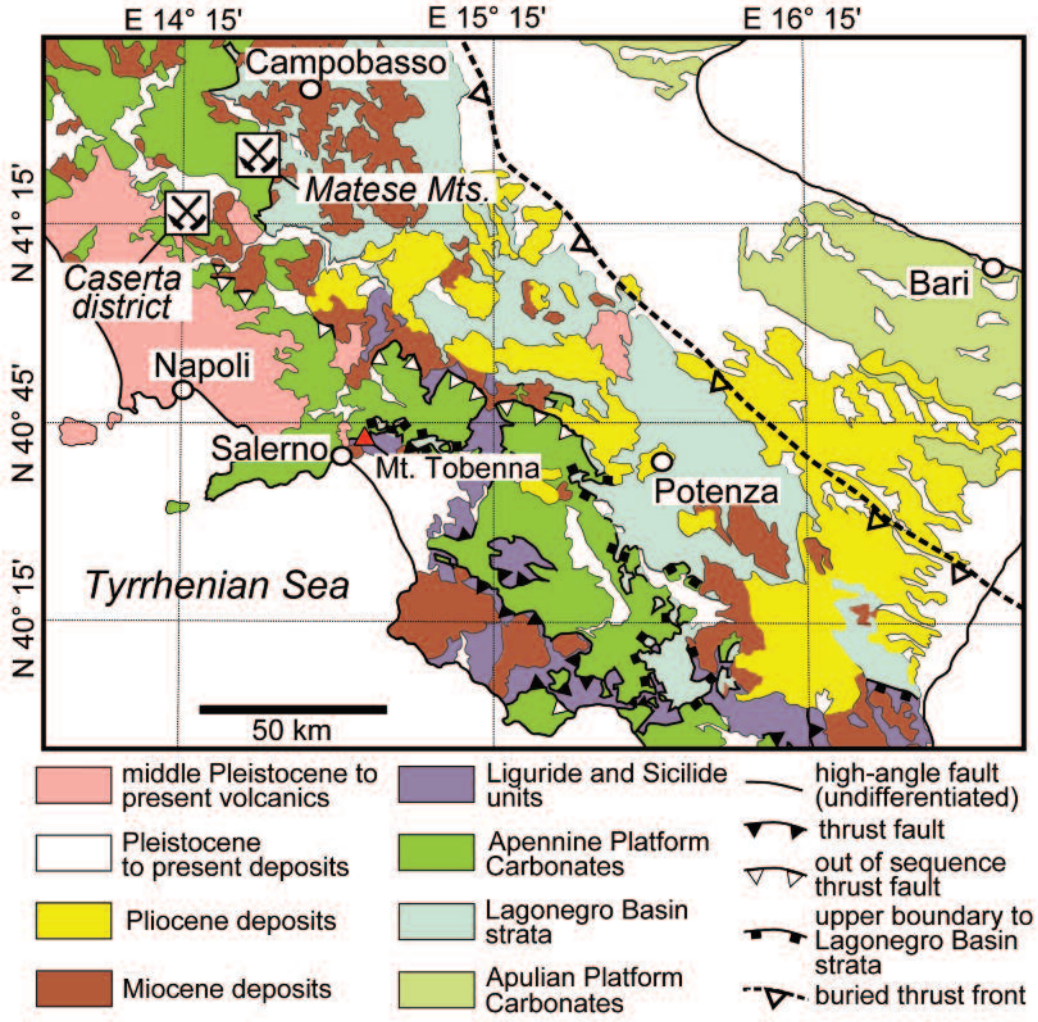

Figure 1. Geological map of southern Italy, with the location of the Matese Mts. and Caserta district bauxite (Bonardi et al., 1988, modified).

Geological setting and bauxite mineralization

The bauxites of the Matese Mts. and the Caserta province are incorporated in a thick Meso-Cenozoic carbonate succession, which builds the main part of the Matese and of the Mt. Maggiore mountain chains (Carannante et al., 2009). These carbonate massifs derive from the deformation of a palaeogeographic domain characterized, from the Triassic to Early Miocene, exclusively by carbonate sedimentation, punctuated by various stratigraphic gaps; these domains correspond to the so-called "Abruzzi-Campania Carbonate

Platform" or "Apennine Carbonate Platform" (Carannante et al., 2009), and are located at the boundary between the Central and Southern Apennines (Figure 1).

The Apennine fold-and-thrust Belt forms part of the Africa-verging mountain system in the Alpine-Mediterranean area. This area evolved within the framework of convergent motion between the African and European plates since the Late Cretaceous (Dewey et al., 1989). Roughly north-south convergence between Africa and Eurasia was dominant up to the Oligocene. During the Neogene, an almost east-directed thrusting toward the Apulian (or Adriatic) continental margin prevailed, associated in the hinterland with the opening of the Tyrrhenian Sea (Malinverno and Ryan, 1986; Royden et al., 1987; Mazzoli and Helman, 1994; Carmignani et al., 2001 and references therein). The Apennine lithotypes consist dominantly of carbonates, shales and cherts (the latter in the basinal sections), ranging in age from Late Triassic to Miocene with substantial facies and thickness variations (Parotto and Praturlon, 1975). The Mesozoic sediments include a platform-dominated succession (Apulian foreland), deeper basinal successions (Umbria-Marche in the northern and Lagonegro in the southern part of the chain), and other so-called "internal" platforms or Apennine Carbonate Platform (Scandone, 1972; D'Argenio et al., 1973; Channell et al., 1979). On the whole, the Apulian foreland and the deformed strata of the Apennines represent a telescoped continental margin with complex sub-basins of differing ages (Mazzoli et al., 2008 and references therein).

The Cretaceous (preorogenic) setting of the Apennine fold-and-thrust Belt has been controversial (Patacca and Scandone, 2007 and references therein). The palaeogeographic map reported in Figure 2 is a summary of the palaeogeographic domains established by Dercourt et al. (1993), and of the plate tectonic model of Schettino and Turco (2011). After these models the Apennine carbonate platform, characterized by shallow-water carbonate sedimentation, was located at tropical latitudes, around 20°N, between the Panormide carbonate platform and the Apulian platform.

During the late Aptian-Coniacian (early Senonian) the Apennine platform, as the Apulian platform were punctuated by repeated and long-lasting emersions, locally testified by bauxite deposits (D'Argenio and Mindszenty, 1995). The varied time-span of the "mid-Cretaceous" stratigraphic gaps supports the hypothesis of a complex tectonically-controlled paleo-topography and of a differential evolution of the related subdomains (Carannante et al., 1994). D'Argenio and Mindszenty (1995) hypothesized that a lithospheric bulge, induced by the early phases of orogenic collision, had been responsible for a long-lived Cretaceous exposure of some sectors of the southern Apennines shelf domain (as in Apulia). More recently, Schettino and Turco (2011), propose instead the existence of a Cretaceous to Cenozoic E-W, left-lateral, strike-slip fault crossing southern Italy, representing the boundary between Adria s.s. and Apulia plates (Figure 2). This fault, operating in a transpressive stress regime, should have induced the uplift of the carbonate platforms and the subaerial exposure. Either way, the subaerial exposures resulted in extensive karstification and, generally, in bauxite deposition (Carannante et al., 1987; Carannante et al., 1994).

The bauxite bodies are unconformably covered by Upper Cenomanian to Coniacian carbonate sediments. Below the unconformity, the limestone is extensively karstified and preserves a complex diagenetic record consisting of multiple events of dissolution, cementation, and internal sedimentation (D'Argenio et al., 1986). In the eastern areas of the Matese Mountains (Regia Piana and Bocca della Selva) the stratigraphic gap extends from Middle-Upper Albian to Turonian-Lower Coniacian (Carannante

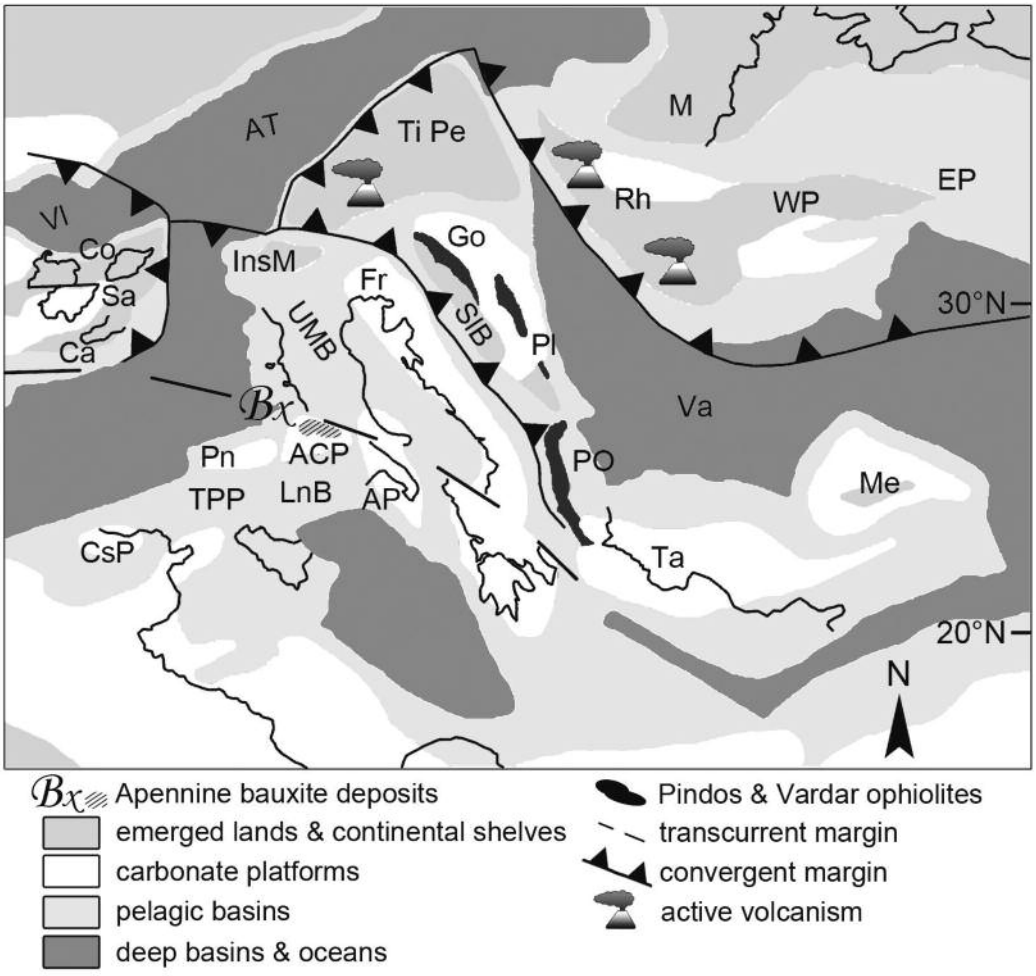

Figure 2. Palaeogeographic map of the Central Mediterranean area during Late Cenomanian; plate margins after Schettino and Turco (2011), paleogeographic domains after Dercourt et al. (1993), modified. ACP = Apennine Carbonate Platform; Ap = Apulian Platform; AT = Alpine Thetys Ocean; Ca = Calabria; Co = Corsica; CsP = Constantine Platform; EP = Eastern Pontides; Fr = Friuli; Go = Goljia Massif; InsM = Insubrian Massif; LnB = Lagonegro Basin; M = Moesia; Me = Menderes; Pe = Pelso; Pl = Pelagonian; Pn = Panormides; PO = Pindos-Olonos; Rh = Rhodope; Sa = Sardinia; SlB = Slovenian Basin; Ta = Taurides; Ti = Tisza; UMB = Umbria-Marches Basin; Va = Vardar; Vl = Valais; WP = Western Pontides.

et al., 2009). In the Caserta district (e.g. Castello di Dragoni), the stratigraphic gap is more limited, covering the transition between Albian and Cenomanian (Carannante et al., 1994). As to the source material of the bauxites, most authors (Bárdossy et al., 1977; D'Argenio et al., 1986; D'Argenio and Mindszenty, 1995) support the idea of possible windblown fine pyroclastics of

acid to intermediate composition, and exclude any contribution from the insoluble residues of the host carbonates.

The bauxite deposits in the Campania district (Matese and Caserta Mountains) form flat, contiguous lenses of a few meters in thickness over shallow karst topography; one exception is the Mt. Maggiore occurrence, where the thickness of the flat bauxite layer sudden increases, e.g. at the Castello di Dragoni mining site to form a sinkhole-fill of about 10 m depth (D'Argenio et al., 1986). The main characteristics of the bauxite deposits, as well as their diagenetic evolution have been widely described in the papers of Crescenti and Vighi (1970), Bárdossy et al. (1977), Carannante et al. (1994) and D'Argenio and Mindszenty (1995).

Sampling and analytical methods

Thirty bauxite samples were collected for the present study from the old deposits of the Matese Mts. (Bocca della Selva and Regia Piana) and of the Caserta province (Dragoni, San Felice, and Maiorano) (Figure 3a, b). Table 1 lists the samples within the considered localities, numbered in a stratigraphic order, from the bottom to the top of each deposit.

X-ray powder diffraction (XRPD) was performed at the Institute of Earth Sciences, Heidelberg University (Germany) with a Siemens D 500 Bragg-Brentano X-ray diffractometer, with Cu$K\alpha$ radiation, 40 kV and 30 mA, 5 s/step and a step scan of 0.05° 2θ. The data were collected from 3 to 110° 2θ. Semiquantitative XRD analyses were performed on all samples. Polished thin sections (~ 30 μm thick) were observed under a petrographic microscope (transmitted and reflected light). SEM examination was carried out using a Jeol JSM 5310 instrument at the University of Napoli (CISAG). EDS microanalyses of mineral phases in thin sections were obtained by the INCA system (Oxford Instruments). Silicates, oxides, and pure elements were used as standards (analytical errors are 1% rel. for major elements, and 3% rel. for minor elements).

Whole rock chemical analyses of major, minor and REE elements for the bauxite samples were carried out at ACME Analytical Laboratories Ltd (Vancouver). The samples were pulverized to 85% - 200 mesh, to obtain about 20 g of pulp. Major oxides and several minor elements were analyzed by ICP-OES following a $LiBO_2$/$Li_2B_4O_7$ fusion and dilute nitric digestion. Loss on ignition (LOI) derives by weight difference after ignition at 1000°C. Rare earth and refractory elements were determined by ICP-MS following a $LiBO_2$/$Li_2B_4O_7$ fusion and nitric acid digestion. In addition, a separate volume split was digested in Aqua Regia and analyzed by ICP-MS to detect the precious and base metals.

QEMSCAN® analysis was carried out at Camborne School of Mines, University of Exeter, UK, using a QEMSCAN® 4300. The QEMSCAN® 4300 is built on a Zeiss Evo 50 SEM platform with four light element Bruker Xflash Silicon Drift energy dispersive X-ray detectors. QEMSCAN® is an automated technique for the rapid characterization of mineral/inorganic species and relationships in polished samples by scanning electron microscopy with energy dispersive X-ray spectrometry (SEM-EDS). The main benefit is the rapid, spatially resolved mineralogical data inferred from chemical spectra (Rollinson et al. 2011), which provide increased information on mineral species, fully quantitative and statistically valid data on ore mineral abundances, particle size and shape distributions, and quantitative data on mineral associations. The basic QEMSCAN® methodology and analytical modes were published by Gottlieb et al. (2000), Pirrie et al. (2004) and Goodall and Scales (2007). The QEMSCAN® software used in this study were iMeasure v. 4.2 for the data acquisition and iDiscover v. 4.2 for the spectral

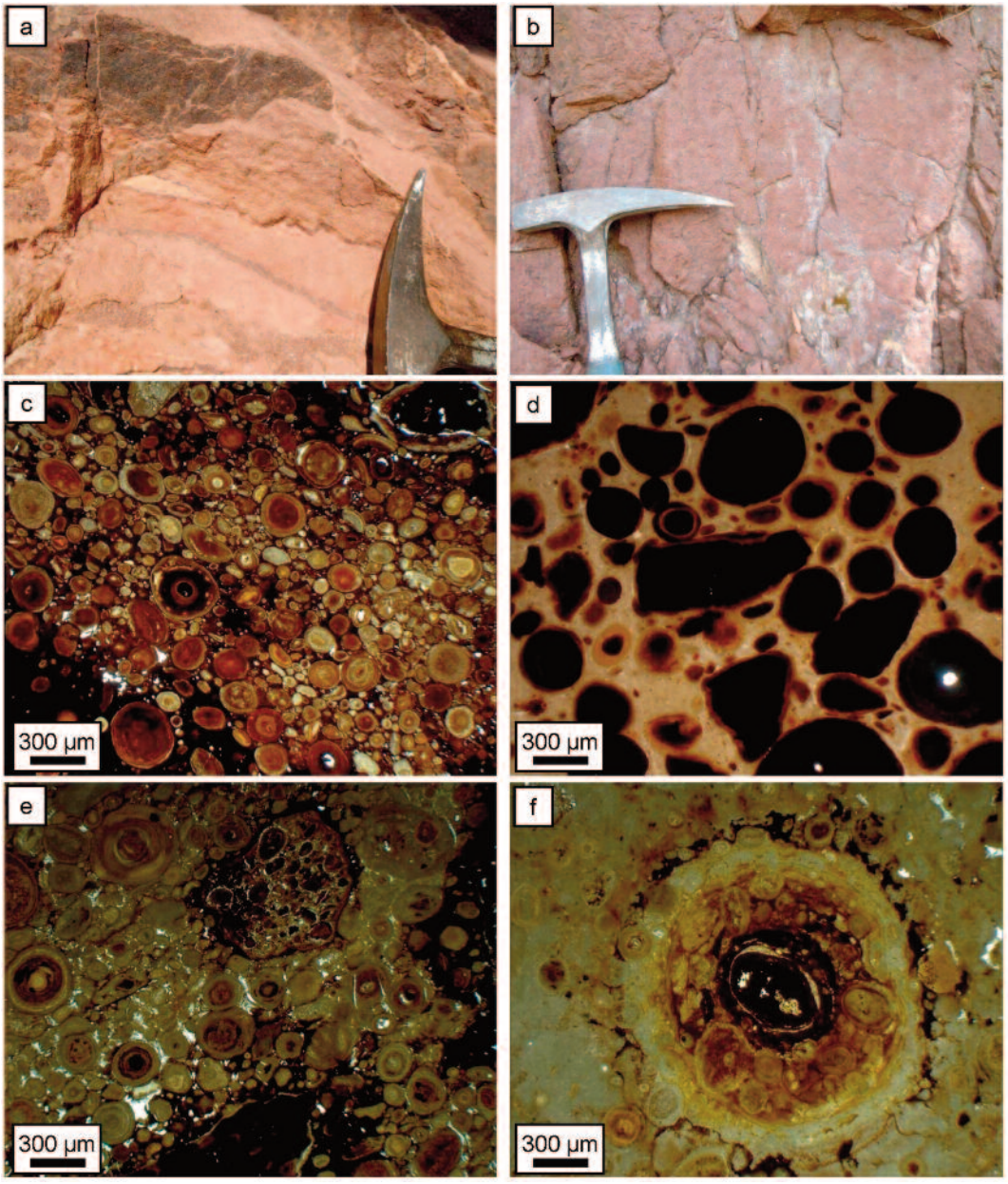

Figure 3. a) Dragoni, thin layering of the massive bauxite body; b) Maiorano, massive bauxite; c) GRBX 16, ooids-supported bauxite, Optical Microscopy (only pol.); d) BXMAI 9, matrix-supported bauxite; angular and rounded hematite/goethite fragments occur, Optical Microscopy (only pol.); e) GRBX 8, a bauxite pebble and ooids of various size, Optical Microscopy (only pol.); f) GRBX 16, composite oolite with a hematite-goethite fragment at the core, Optical Microscopy (only pol.). Label samples as in Table 1.

Table 1. Samples within the considered localities, numbered in stratigraphic order, from the bottom to the top of the deposit.

Matese Mts. district	Regia Piana	profile 1	GRBX 1
			GRBX 2
			GRBX 3
		profile 2	GRBX 4
			GRBX 5
			GRBX 6
		profile 3	GRBX 7
			GRBX 8
			GRBX 9
			GRBX 10
			GRBX 11
			GRBX 12
			GRBX 13
		profile 4	GRBX 14
			GRBX 15
			GRBX 16
	Bocca della Selva	profile 1	GRBX 17
			GRBX 18
Caserta district	San Felice	profile 1	BXRA 1
			BXRA 2
	Dragoni	profile 1	BXDRA 1
			BXDRA 2
			BXDRA 3
			BXDRA 4
			BXDRA 5
			BXDRA 6
			BXDRA 7
	Maiorano	profile 1	BXMAI 8
			BXMAI 9
			BXMAI 10

interpretation and data processing. The fieldscan measurement mode was used to collect X-ray data every 10 μm across the polished sample surfaces of the thin sections, with X-rays acquired at 1000 total X-ray counts per spectrum. For this study the LCU5 SIP provided with the QEMSCAN® (containing common minerals) was modified to include the bauxite mineral components.

Mineralogy and Petrography

The texture of the bauxite samples was studied in thin sections by optical microscope and

electron microscopy. The texture is mainly oolitic to pisolitic (Figure 3c) and generally "impure", due to the occurrence of Al(-Fe) hydroxides together with almost ubiquitous clays in the matrix. It can also change from purely oolitic to arenitic-conglomeratic, suggesting reworking of evolved lateritic soils. Abundant angular fragments of hematite-goethite occur as mm-sized clasts in the bauxite of Bocca della Selva, Dragoni and Maiorano (Figure 3d). In the Regia Piana deposit the amount and sizes of the detrital fragments are variable. The texture of the bauxite can be ooids-supported (Figure 3c) or matrix-supported (Figure 3d), and it is possible to find locally graded-bedded levels. The cores of the ooids generally consist of older, detrital bauxite grains (bauxite pebbles, Figure 3e), or of hematite-goethite fragments (Figure 3f). There are differences in the mineral distribution between the ooids and the groundmass. Generally, boehmite and hematite seem to be more abundant in the ooids, whereas kaolinite is (generally secondarily) enriched in the groundmass. However, in the structure of most ooids, boehmite and kaolinite are zoned, following a well-known diagenetic pattern (Bárdossy, 1982).

The results of semiquantitative XRD analysis of 15 representative samples are summarized in Table 2. Mineral composition of bulk bauxite samples does not change significantly among the deposits pertaining to the two mining areas (Bocca della Selva and Regia Piana in Matese Mts.; Dragoni, San Felice, and Maiorano in the Caserta district), but the relative mineral proportions vary in relation to the position of the samples within the deposit. Boehmite (50-75 wt.%) is the main Al-rich mineral, with higher percentages in the bauxites of Bocca della Selva and those of the Caserta mining district. Silica-bearing phases are mostly clay minerals, the most important being kaolinite (3-20 wt.%, with higher contents in the Matese Mts. bauxites). In the Caserta district, traces of illite/smectite also occur. Gibbsite has been detected only in few samples (GRBX 3, BXDRA 3 and BXDRA 6). Hematite is the main Fe-bearing mineral, averaging about 15 wt.% in both districts. Goethite can also occur, locally in higher amounts than hematite, as well as minor lepidocrocite. Anatase is quite ubiquitous, varying around 7 and 10 wt.%. In some samples (e.g. BXRA 1, San Felice profile), traces of zircon and monazite have been recorded in the XRD patterns.

Two representative samples from the Caserta district (BXDRA 6, Dragoni profile, and BXMAI 8, Maiorano profile) have been analyzed with QEMSCAN® using fieldscan mode (Figure 4). This new type of analysis allows a high resolution chemical-mineralogical map of a whole thin section to be produced, with different degrees of detail and different "chemical" resolution, as well as the modal quantitative evaluation of the identified phases. In the QEMSCAN® images of Figure 4a it is possible to see a large-scale chemical-mineralogical map of the thin sections. In both sections analyzed three main mineralogical phases have been detected: Al-hydroxides, Fe-Al-hydroxides and Fe-hydroxides, which should correspond to pure boehmite, mixed Fe-rich boehmite/Al-rich goethite and pure goethite. In the Maiorano BXMAI 8 sample, some clay minerals were also detected. In the images of Figure 4b, more detailed maps of the two sections are shown. In the sample BXDRA 6 the mineral composition is dominated by Al-hydroxides (e.g. boehmite) that vary from pure (42 wt.%) to Fe-rich (34 wt.%) types. Al-bearing goethite (15 wt.%) and goethite (6 wt.%) occur, together with minor calcite (2 wt.%) and clay minerals (kaolinite and montmorillonite, 1 wt.%). The mineralogy of BXMAI 8 is dominated by Fe-rich Al-hydroxides (50 wt.%), with a reduced amount of pure Al-hydroxides (10 wt.%). Hematite (12 wt.%), goethite (2 wt.%), clay minerals (montmorillonite and kaolinite, 11 wt.%) and Al-bearing goethite (14 wt.%) account for the rest of dominant minerals. The relative

Table 2. Relative abundance of minerals in selected bauxite samples (semiquantitative XRD).

		Boehmite	Gibbsite	Diaspore	Goethite	Hematite	Lepidocrocite	Anatase	Kaolinite	Illit./Mont.	Calcite	Rutile	Quartz	Zircon	Monazite
Matese Mts. District	GRBX3	OOOO	OO	O	OO	O	-	OO	OO	-	-	O	-	-	-
	GRBX7	OOOOO	-	-	OO	O	O	OO	OO	-	-	O	-	-	-
	GRBX8	OOOOO	-	-	O	O	-	OO	OO	-	-	-	-	-	-
	GRBX14	OOOOO	-	-	-	O	-	OO	OO	-	-	-	-	-	-
	GRBX16	OOOOO	-	-	-	OO	-	OO	OO	-	-	O	-	-	-
	GRBX17	OOOOO	-	-	-	OOO	-	O	-	-	-	O	O	-	-
	GRBX18	OOOOO	-	-	O	OO	-	OO	-	-	-	-	-	-	-
Caserta district	BXRA 1	OOOO	-	-	-	OOO	OO	O	O	O	-	-	-	O	O
	BXDRA 3	OOO	O	-	O	O	-	O	O	O	OOOO	O	-	-	-
	BXDRA 4	OOOOO	-	-	-	OO	-	O	O	O	-	O	-	-	-
	BXDRA 5	OOOOO	-	-	-	OO	-	O	-	O	-	O	-	-	-
	BXDRA 6	OOOOO	O	-	OO	OO	-	OO	O	O	-	O	-	O	O
	BXMAI 8	OOOOO	-	-	-	OO	O	O	O	O	-	O	-	-	-
	BXMAI 9	OOOOO	-	-	O	OO	O	O	O	O	-	O	-	-	-
	BXMAI 10	OOOOO	-	-	-	OO	O	O	O	O	-	O	-	-	-

- not found, O <5 wt.%, OO 5-20 wt.%, OOO 20-40 wt. %, OOOO 40-60 wt. %, OOOOO > 60 wt.%

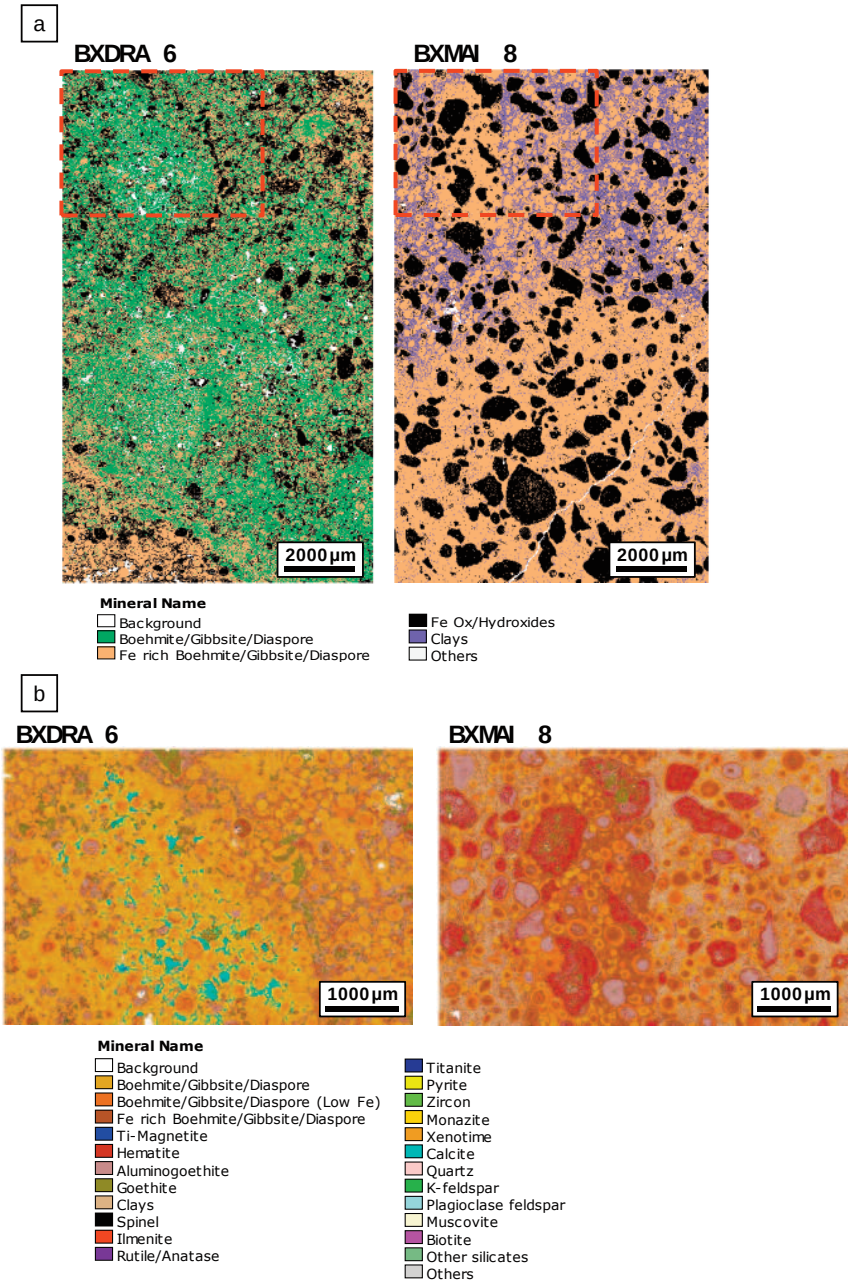

Figure 4. False colour fieldscan images of the thin section samples (QEMSCAN®). a) BXDRA 6 and BXMAI 8, thin section large scale chemical-mineralogical maps, main phases; b) enlargements of a), detailed chemical-mineralogical maps, all detected phases are indicated in the legend.

amounts of the mixed hydroxides were classified as boehmite or goethite, based on the relative major content of Al or Fe, respectively measured in the phase. It is clear that the BXDRA 6 section is more enriched with Al-phases than BXMAI 8, which contains more Fe. Considering the textural characteristics highlighted by QEMSCAN® (Figure 4a, b), we see that the sample BXMAI 8 seems to be mainly matrix-supported, whereas the sample BXDRA 6 mainly ooids-supported. In the sample BXMAI 8, we can observe that the clays occur mainly in the matrix, together with Fe-rich Al-hydroxides, and hematite occurs preferentially in the angular mm-sized fragments, coated at the rim by boehmite and/or goethite. The angular hematite-goethite fragments have variable size and roundness. In the sample BXDRA 6, the ooids consist mainly of pure Al-hydroxides, with only thin rims of low-Fe phases; the matrix consists mainly of clays, Fe-rich Al-hydroxides and Fe-hydroxides.

By means of SEM-EDS analysis, we have been able to detect a large number of tiny detrital minerals (size ranges 5 - 100 μm) both in the ooids and in the matrix of bauxite (Figure 5). Some of them were already mentioned in Bárdossy et al. (1977). The most frequent is zircon, which is commonly Hf-rich, but can also contain Sc and Ca. Rutile, monazite and ilmenite have also been commonly detected, together with minor xenotime, and titanomagnetite. Rutile and ilmenite maintain often a euhedral-subhedral habitus, whereas zircon and monazite are slightly rounded. We found also small clusters of not previously detected qandilite $[(Mg, Fe^{2+})_2(Ti, Fe^{3+}, Al)\ O_4]$, and of hercynite-type spinels. We were able to detect with QEMSCAN® also other detrital minerals occurring in traces in the samples, beyond those already found with SEM-EDS. These are: quartz, feldspar, muscovite (< 15μm), spinel (incl. Cr-spinel), olivine**,** titanite and a Mg-bearing phyllosilicate (serpentine/talc?).

Geochemistry

Whole-rock major and trace element concentrations of representative samples from the Matese Mt. and Caserta district bauxite are given in Table 3.

As expected, the Al_2O_3 and Fe_2O_3 contents are relatively high in all samples (on average, 54.07 wt.% and 23.53 wt.% respectively), and SiO_2 and TiO_2 have average values of 5.50 wt.% and 2.68 wt.%, respectively. LOI has been evaluated around 13.15 wt.%. The Al_2O_3 content of the Matese Mts. bauxite varies between values of 46.03-48.57 wt.% at the Bocca della Selva deposit and of 67.52 wt.% at the Regia Piana deposit. In the Caserta mining district, the San Felice bauxite is relatively poor, with only 36.75 wt.% Al_2O_3, whereas at Dragoni, values around 50 wt.% of Al_2O_3 have been reached.

In the Matese Mts., Fe_2O_3 is higher at Bocca della Selva (35.39-38.95 wt.%), and has its minimum values in one of the Regia Piana samples (about 10 wt.%). In the bauxite samples of the Caserta district, Fe_2O_3 is comprised between 24.70 wt.% and 40.84 wt.%. In the Matese Mts. deposits the lowest SiO_2 values have been detected at Bocca della Selva (about 1.5 wt.%), whereas amounts between 4 wt.% and 11 wt.% SiO_2 have been measured in the Regia Piana bauxite. In the Caserta district, SiO_2 varies between 2 wt.% and 5 wt.% in both the Dragoni and Maiorano bauxite, whereas is high (about 9 wt.%) in the San Felice sample. The oxides of other major elements have an average amount below 0.5 wt.%.

It is also important to consider the amount of the so-called "*bauxitophile*" minor elements (Table 3), i.e. Cr (up to 0.07 wt.%), Ni (up to 400 ppm), V (up to 730 ppm), Co (118 ppm) and, of course, Zr (up to 600 ppm). Cr has higher values in the Maiorano, Dragoni and Bocca della Selva deposits than in Regia Piana and San Felice bauxites. Ni is strongly enriched in the Maiorano deposit, whereas it remains variable on mean

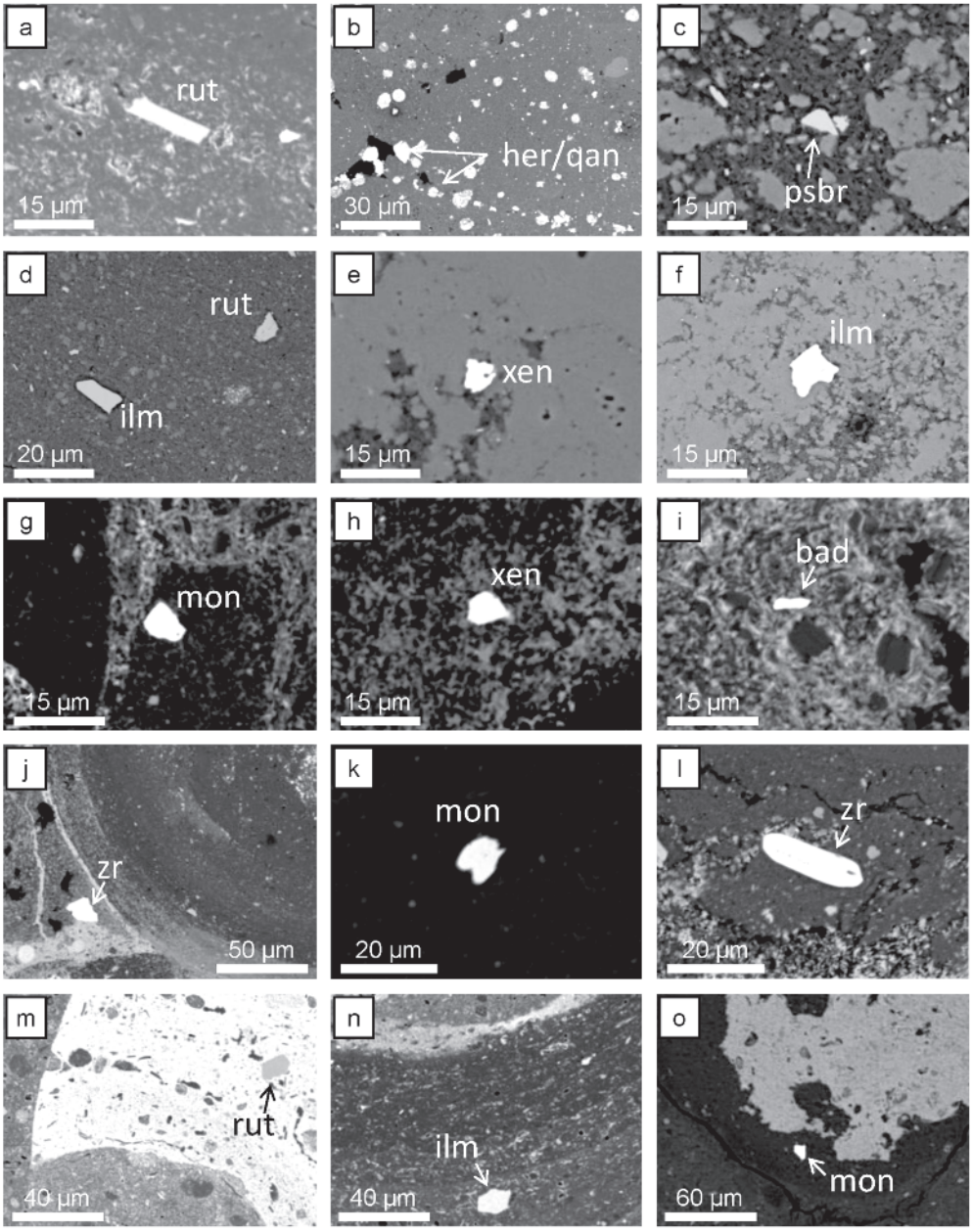

Figure 5. Backscattered electrons images (BSE) of detrital minerals in the Campania bauxites. a) GRBX 18, rutile; b) GRBX 15, hercynite/qandilite; c) GRBX 2, pseudobrookite; d) GRBX 2, ilmenite and rutile; e) GRBX 2, xenotime; f) GRBX 2, ilmenite; g) BXRA 1, monazite; h) BXRA 1, xenotime; i) BXRA 1, baddeleyite; j) BXRA 1, zircon; k) BXDRA 6, monazite; l) BXDRA 6, zircon; m) BXMAI 8, rutile in a Fe-rich ooid core; n) BXMAI 8, ilmenite in an Al-rich ooid rim; o) BXMAI 8, monazite in an Al-rich crust.

Table 3. Major (wt. %) and selected trace elements (ppm) composition of representative bauxite samples.

	Regia Piana									
	GRBX 3	GRBX 4	GRBX 7	GRBX 8	GRBX 9	GRBX 12	GRBX 13	GRBX 14	GRBX 15	GRBX 16
SiO_2	11.21	6.86	7.15	7.26	6.52	8.05	10.96	3.82	3.69	4.37
TiO_2	2.40	3.05	2.76	2.96	3.31	2.48	2.67	3.38	3.06	3.06
Al_2O_3	52.59	63.00	62.18	58.63	62.98	50.50	54.68	67.52	62.50	64.34
Fe_2O_3	14.69	9.99	10.84	17.39	11.60	26.01	14.72	10.48	16.93	14.34
MnO	0.03	0.05	0.04	0.04	0.04	0.04	0.03	0.05	0.04	0.04
MgO	0.22	0.22	0.20	0.19	0.22	0.20	0.20	0.13	0.11	0.13
CaO	0.10	0.15	0.13	0.10	0.12	0.17	0.30	0.06	0.10	0.08
Na_2O	0.05	0.04	0.04	0.04	0.03	0.05	0.05	0.02	0.03	0.02
K_2O	0.17	0.15	0.10	0.11	0.11	0.12	0.16	0.05	0.04	0.05
P_2O_5	0.12	0.03	0.09	0.07	0.09	0.11	0.14	0.05	0.06	0.05
Cr_2O_3	0.05	0.06	0.06	0.06	0.07	0.05	0.06	0.06	0.06	0.06
LOI	17.90	16.10	16.10	12.80	14.60	11.80	15.60	14.20	13.10	13.20
Total	99.61	99.77	99.74	99.71	99.71	99.62	99.57	99.79	99.76	99.77
V	293.0	294.0	328.0	440.0	421.0	462.0	321.0	346.0	398.0	352.0
Co	37.8	19.3	22.4	23.1	21.8	22.3	39.6	18.2	19.2	26.6
Ni	243.0	163.0	174.0	174.0	154.0	159.0	246.0	82.0	93.0	103.0
Cu	12.8	9.3	10.9	8.9	10.3	11.4	13.9	7.9	6.2	12.0
Zn	14.0	21.0	12.0	14.0	18.0	17.0	13.0	9.0	12.0	14.0
Sr	273.7	39.8	249.6	79.5	76.6	59.1	328.1	77.3	84.2	82.5
Y	48.3	57.1	57.6	64.0	62.3	78.8	52.1	54.6	51.8	50.2
Zr	477.5	523.6	499.3	570.7	596.1	519.3	534.7	545.7	505.2	524.3
Nb	49.0	62.0	54.2	56.2	65.1	48.7	56.0	65.2	60.2	61.5
Ba	42.0	39.0	30.0	21.0	17.0	24.0	47.0	15.0	17.0	14.0
Hf	15.8	16.4	15.6	18.5	19.3	16.3	17.1	18.4	16.5	15.9
Pb	156.2	33.4	44.1	128.3	16.4	190.2	173.7	27.8	48.9	37.0
La	308.5	67.1	79.9	87.7	66.7	108.7	354.7	45.1	52.1	45.3
Ce	712.6	131.6	155.0	154.1	220.7	693.1	828.1	104.8	115.1	90.6
Pr	51.7	16.4	18.5	19.8	17.9	32.8	55.3	11.0	13.5	11.0
Nd	155.2	62.1	69.1	74.2	67.4	129.1	151.0	42.7	51.3	46.0
Sm	16.9	11.4	12.9	13.4	12.8	27.0	15.7	7.9	10.4	8.5
Eu	3.1	2.4	2.6	2.9	2.6	5.9	2.7	1.7	2.2	1.8
Gd	14.4	10.4	11.2	12.0	11.6	27.1	14.6	7.9	9.4	8.2
Tb	2.0	1.9	1.9	2.1	1.9	4.0	2.0	1.5	1.7	1.5
Dy	10.1	10.7	11.1	11.9	11.4	20.6	11.3	9.4	9.8	9.3
Ho	2.0	2.2	2.3	2.5	2.3	3.8	2.2	2.1	2.1	1.9
Er	6.2	6.8	7.1	7.7	7.1	10.3	6.6	6.1	6.3	5.9
Tm	1.1	1.2	1.2	1.3	1.2	1.7	1.1	1.1	1.1	1.0
Yb	7.2	8.2	7.8	8.4	7.9	10.9	7.8	7.0	7.3	6.6
Lu	1.1	1.3	1.3	1.3	1.2	1.7	1.2	1.1	1.1	1.0
Th	100.1	57.8	60.0	87.2	83.0	86.6	113.0	58.8	41.6	46.7
U	26.1	18.7	6.1	7.8	5.9	11.4	26.4	8.2	12.8	11.5
$(La/Yb)_{ch}$	28.81	5.54	6.90	7.06	5.70	6.70	30.78	4.36	4.84	4.60
Ce/Ce*	1.18	0.91	0.91	0.83	1.51	2.81	1.21	1.07	1.01	0.91
Eu/Eu*	0.60	0.68	0.67	0.69	0.64	0.67	0.55	0.64	0.68	0.66

- = below detection limit $(La/Yb)_{ch}=(La/La_{ch})/(Yb/Yb_{ch})$ $Ce/Ce^*=(3Ce/Ce_{ch})/(2La/La_{ch}+Nd/Nd_{ch})$ $Eu/Eu^* = Eu_{ch}/\sqrt{(Sm_{ch}\bullet Gd_{ch})}$

Table 3. Continued...

	Bocca della Selva		*San Felice*	*Dragoni*			*Maiorano*		
	GRBX 17	GRBX 18	BXRA 1	BXDRA 4	BXDRA 5	BXDRA 6	BXMAI 8	BXMAI 9	BXMAI 10
SiO_2	1.54	1.66	9.13	5.12	2.24	3.34	3.64	4.49	3.53
TiO_2	2.50	2.55	2.01	2.50	2.44	2.62	2.20	2.44	2.54
Al_2O_3	46.03	48.57	36.75	51.09	48.78	53.22	42.55	50.04	51.44
Fe_2O_3	38.95	35.39	37.97	28.72	33.17	24.70	40.84	29.99	30.27
MnO	0.23	0.22	0.07	0.20	0.22	0.09	0.25	0.18	0.23
MgO	0.06	0.07	0.28	0.14	0.15	0.21	0.13	0.25	0.20
CaO	0.05	0.08	0.28	0.19	0.93	0.23	0.13	0.11	0.10
Na_2O	-	0.03	0.04	0.03	0.03	0.05	0.03	0.03	0.03
K_2O	-	0.01	0.37	0.07	0.02	0.09	0.07	0.15	0.09
P_2O_5	0.05	0.04	0.13	0.05	0.05	0.09	0.04	0.05	0.04
Cr_2O_3	0.08	0.07	0.06	0.07	0.07	0.08	0.09	0.07	0.07
LOI	10.20	11.00	12.60	11.50	11.60	14.90	9.70	11.90	11.10
Total	99.70	99.71	99.68	99.75	99.73	99.64	99.70	99.72	99.72
V	342.0	282.0	732.0	244.0	288.0	406.0	465.0	341.0	316.0
Co	33.3	31.8	32.7	37.2	40.8	118.6	50.8	46.4	41.4
Ni	126.0	132.0	143.0	225.0	158.0	253.0	416.0	354.0	276.0
Cu	55.6	54.7	81.1	72.0	45.6	332.9	69.2	83.2	37.9
Zn	63.0	62.0	44.0	81.0	67.0	68.0	65.0	76.0	54.0
Sr	32.9	35.6	102.7	40.8	31.2	44.4	32.9	41.0	32.7
Y	58.8	61.0	51.5	75.8	73.4	67.7	67.3	108.8	71.7
Zr	493.5	487.9	385.2	432.9	462.6	449.9	428.4	441.4	438.5
Nb	47.5	49.2	36.1	43.7	47.0	47.8	39.8	45.3	44.9
Ba	28.0	31.0	47.0	26.0	33.0	26.0	33.0	30.0	30.0
Hf	16.5	14.3	11.4	12.0	13.5	12.7	13.6	12.0	12.1
Pb	155.9	117.1	171.2	97.6	122.5	146.4	139.1	101.5	105.3
La	107.2	106.0	102.0	114.0	129.3	135.2	146.7	125.9	125.4
Ce	232.4	278.3	231.4	230.9	325.4	392.8	320.5	233.8	390.9
Pr	24.6	24.1	27.2	28.4	31.5	39.1	33.3	29.6	34.3
Nd	89.0	92.4	101.8	106.7	117.2	149.7	126.4	109.5	125.4
Sm	16.6	16.9	17.7	19.8	21.0	27.9	22.6	20.8	23.6
Eu	3.5	3.6	3.6	4.2	4.4	5.6	4.7	4.6	4.8
Gd	13.7	14.6	14.5	17.3	17.5	21.8	18.9	21.2	18.5
Tb	2.3	2.4	2.1	2.9	2.8	2.9	2.9	3.3	2.8
Dy	12.9	13.0	10.8	16.4	15.3	13.7	15.9	19.0	16.2
Ho	2.4	2.6	1.9	3.3	3.1	2.5	3.0	3.8	2.9
Er	6.9	7.9	5.3	9.7	9.1	7.3	9.1	10.9	8.5
Tm	1.2	1.3	0.8	1.4	1.3	1.1	1.4	1.5	1.3
Yb	7.5	7.9	5.4	9.1	8.6	7.4	8.8	9.8	8.9
Lu	1.1	1.2	0.8	1.4	1.3	1.2	1.4	1.5	1.3
Th	68.5	53.6	35.3	46.3	58.2	51.9	64.3	50.4	51.8
U	5.1	4.5	18.4	5.4	5.4	16.4	5.6	5.6	5.6
$(La/Yb)_{ch}$	9.65	9.02	12.66	8.44	10.18	12.25	11.19	8.63	9.52
Ce/Ce*	1.03	1.23	1.04	0.94	1.17	1.30	1.03	0.87	1.43
Eu/Eu*	0.72	0.70	0.69	0.70	0.71	0.70	0.69	0.66	0.69

- = below detection limit $(La/Yb)_{ch}=(La/La_{ch})/(Yb/Yb_{ch})$ $Ce/Ce^*=(3Ce/Ce_{ch})/(2La/La_{ch}+Nd/Nd_{ch})$ $Eu/Eu^* = Eu_{ch}/\sqrt{(Sm_{ch}\bullet Gd_{ch})}$

values in the other bauxites. V is very high in the San Felice sample, whereas it shows mean values (~ 300-400 ppm) in the other deposits. Co has an anomalous high value (118 ppm) in a Dragoni sample, whereas remains on lower amounts in the other analyzed bauxites; in general, it is slightly higher in Maiorano and Dragoni deposits than other sites. Zr shows higher values in the Matese district bauxites than in the Caserta Mt. deposits. Anomalous Cu (up to 330 ppm) and Pb (up to 170 ppm) values have also been detected.

In the diagrams of Figure 6a, we can see that Al_2O_3 and SiO_2 display a negative correlation for the Regia Piana bauxite. Fe_2O_3 decreases continuously in all the samples while Al_2O_3 is increasing (Figure 6b). TiO_2 has a perfect positive correlation with Al_2O_3 (Figure 6c). Cr_2O_3 shows a positive correlation with Al_2O_3 only in the Regia Piana bauxite, while in the other deposits the Cr_2O_3 values are higher, but not correlated with those of Al_2O_3 (Figure 6d).

It is important to consider that the Regia Piana deposit has the highest alumina content, compared to the other deposits. The Bocca della Selva bauxite, also pertaining to the Matese Mts. district, has a chemical composition much similar to that of the Dragoni and Maiorano bauxites (Caserta district). This can be observed in the SiO_2/Al_2O_3 and Cr_2O_3/Al_2O_3 correlation diagrams (Figure 6a and d), where the Bocca della Selva bauxite clusters with the bauxite samples of the Caserta mining district.

REE concentrations in the bauxites of the Matese Mts. and the Caserta district are shown in Table 3. Eu vs Gd and Ce vs Nd diagrams are shown in Figure 6e and f. A positive correlation between Eu and Gd is established (Figure 6e), with an almost constant Eu/Gd ratio. This is due to the similar behavior of these two elements during weathering. Ce and Nd show again a positive correlation, but the ratio is more variable (Figure 6f), and there are also three samples (GRBX 3, GRBX12 and GRBX 13) where the Ce content is very high. Mongelli (1997 and references therein) has shown that cerium oxidation from Ce^{3+} to Ce^{4+} causes a strong decrease of the element mobility, and, in general, the precipitation of Ce-oxidized minerals, e.g., cerianite, bastnasite. He has also demonstrated that cerium oxidation in the Apulian bauxites occurs preferentially in the higher part of the bauxite profile, and creates a "positive anomaly" among other REEs. Our three Ce-anomalous samples confirm this "rule", having been collected from the highest stratigraphic horizons of the Regia Piana bauxite.

In the PAAS (Post-Archean Australian Shale)-normalized REE pattern (Figure 7a), it is possible to observe the behavior of the rare earth elements during the weathering and formation of bauxites. The REE contents are higher in the Caserta district bauxites than in the Matese Mts., with the exception of the GRBX 3, GRBX 12 and GRBX 13 samples (located at the top of the profile in the Regia Piana deposit). The sample GRBX 12 has a pronounced Ce anomaly, evidenced also by the high Ce/Ce* ratio. The samples GRBX 3 and GRBX 13 have a Ce/Ce* ratio similar to other samples, but they show a very high $(La/Yb)_{ch}$ ratio, differently from all others (Figure 7b). The anomalous enrichment of cerium and other LREE in these samples can be related to the occurrence of minerals of the bastnäsite group (Bárdossy et al., 1977), as well as, to the occurrence of authigenic Ce-high, La-Nd-low phosphate minerals, containing also Ca, probably deriving from local weathering of monazite (Figure 8).

Most samples from the Matese Mts. have maximum REE contents three times higher than the PAAS (Figure 7a), with the Bocca della Selva samples (GRBX 17, GRBX 18) more enriched in REE than the Regia Piana samples. At Bocca della Selva the PAAS-normalized LREE and HREE patterns seem to be the same, whereas in most of the samples of the Regia Piana deposit the HREE are slightly more enriched than LREE.

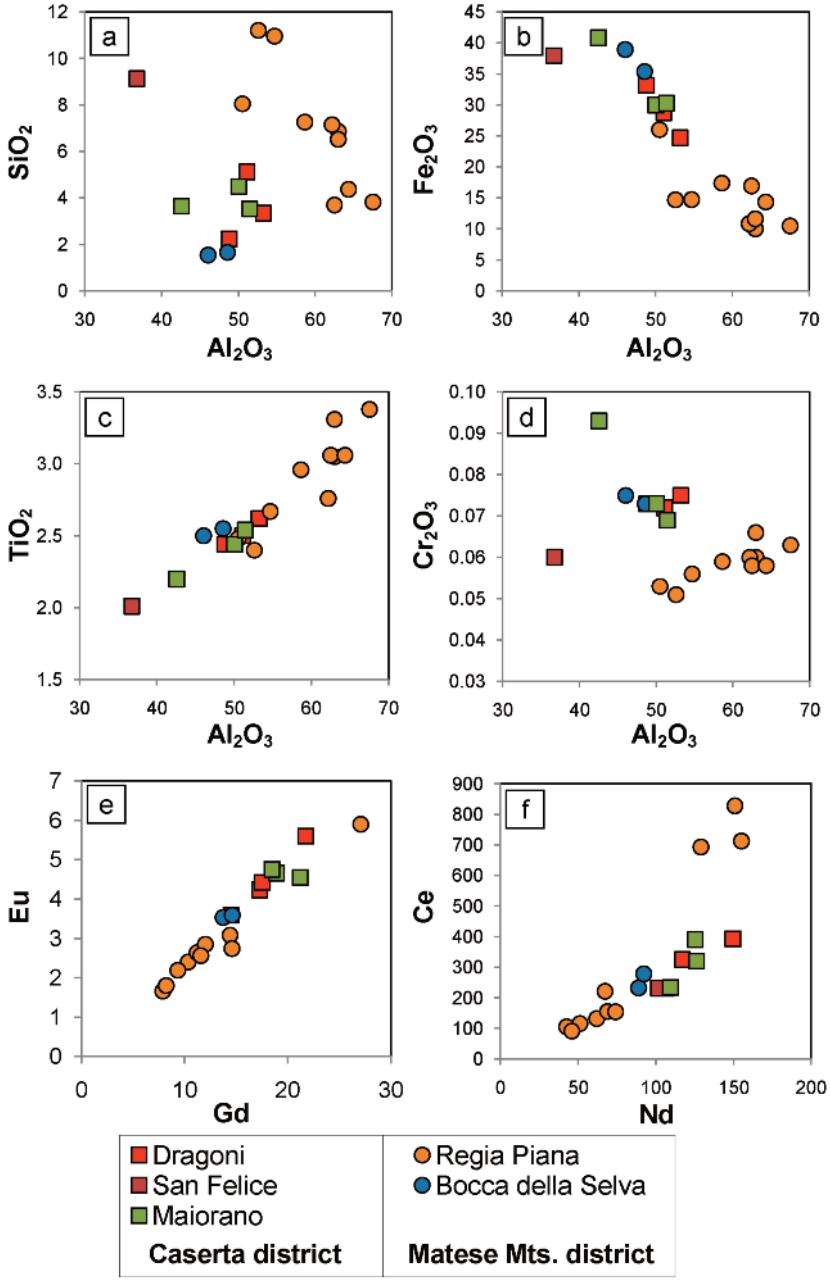

Figure 6. a) Binary diagrams showing the correlation between Al_2O_3 and SiO_2, b) Fe_2O_3, c) TiO_2, and d) Cr_2O_3 values, and e) Gd vs Eu, and f) Nd vs Ce values, for the analyzed deposits. Al_2O_3 and SiO_2, Fe_2O_3, TiO_2 and Cr_2O_3 are in wt.%, Gd, Eu, Nd and Ce are in ppm. Matese Mts. district = circles; Caserta district = squares.

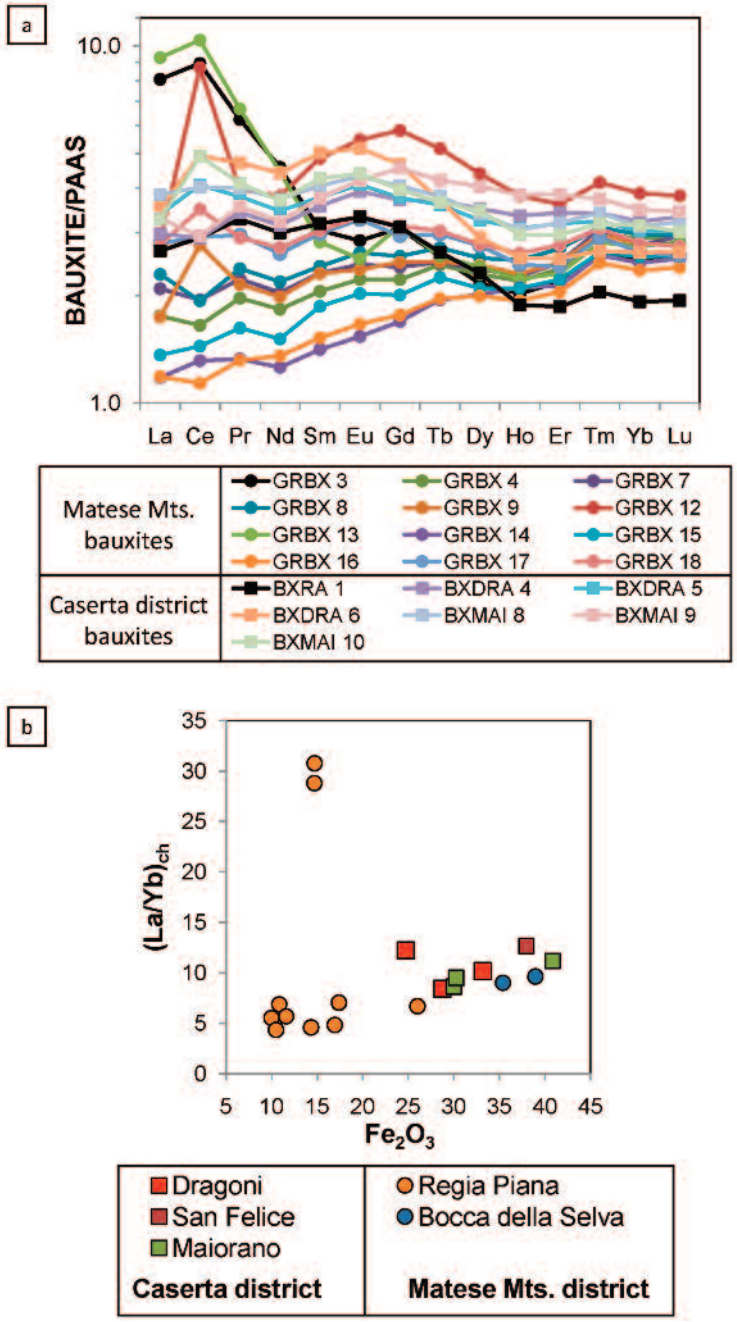

Figure 7. a) PAAS-normalized REE patterns. b) $(La/Yb)_{ch}$ ratio vs Fe_2O_3 (wt.%) binary diagram. Matese Mts. district bauxites are indicated with circles, Caserta district bauxites are indicated with squares.

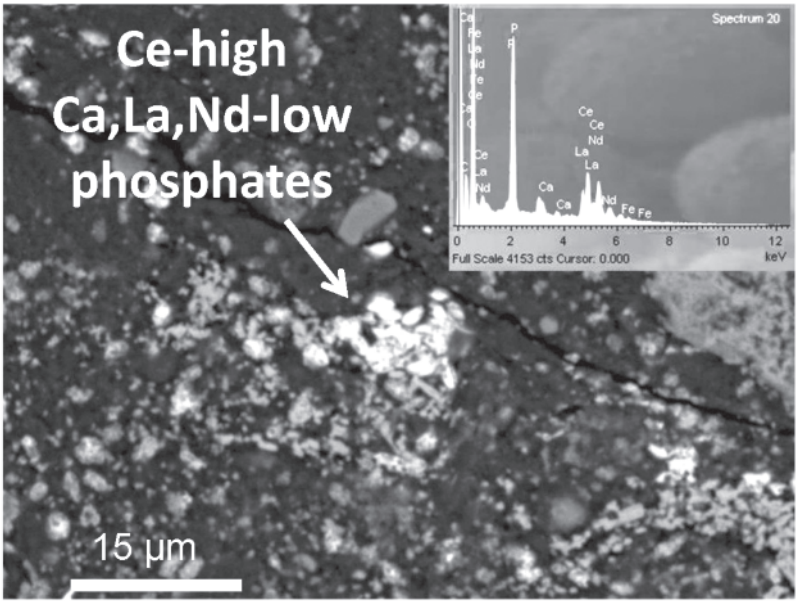

Figure 8. Backscattered electrons image (BSE) of authigenic REE-phosphates in the sample GRBX 12: Ce_2O_3 45-56 wt.%, La_2O_3 0-4 wt.%, Nd_2O_3 2-7 wt.%, CaO 5-6 wt.%.

The Caserta district bauxites, as mentioned, are more enriched in REE than the Matese Mts. deposits. The samples have REE amounts between three and six times higher than PAAS. There are two samples (BXRA 1 and BXDRA 6), in which the LREE/HREE ratio is higher than in the other samples; this may be related to the occurrence in the two samples of anomalous amounts of monazite. These observations are reflected in the values of the $(La/Yb)_{ch}$ ratio (Table 3; Figure 7b). In the Caserta district $(La/Yb)_{ch}$ ratio is higher than in the Matese Mts. deposits, testifying a major enrichment of LREE on HREE in the former than in the second. Within the Matese Mts. district, the $(La/Yb)_{ch}$ ratio is higher in the Bocca della Selva bauxite than Regia Piana deposit. Within the Caserta district, the $(La/Yb)_{ch}$ ratio is higher in the samples BXRA 1 and BXDRA 6, than in the others, confirming the preliminary observation deriving from the PAAS-normalized diagram. Moreover, in the diagram of Figure 7b, it is possible to see that a positive correlation exists between $(La/Yb)_{ch}$ ratio and Fe_2O_3. Bocca della Selva deposit has REE geochemical characteristics more similar to the Caserta district bauxites than Regia Piana deposit.

Discussion

Genetic process

The ore textures of the studied bauxites, as also mentioned in Bárdossy et al. (1977) and D'Argenio et al. (1986), range between oolitic to oolitic-conglomeratic and arenitic in all the deposits. Numerous bauxite grains/pebbles and hematite-goethite angular fragments occur among the ooids. This suggests that at least part of the material occurring in the actual deposits derives from the erosion of older bauxites, formed elsewhere on the exposed carbonate platform. A multiple reworking of the original

lateritic soils seems to have occurred, with transport and widespread deposition of the bauxite material on a karst landscape; therefore in the studied deposits it has never been possible to find a typical lateritic bauxite profile in situ on an alumosilicate protore.

By QEMSCAN® analysis we could observe additional textural details, regarding the diagenesis of the bauxite ore. The Al-hydroxides tend to be more concentrated in the ooids, following multistep concentric patterns, in which also detrital components (e.g. Fe-rich duricrust fragments and bauxite pebbles) are coated with rims consisting of Al-hydroxides. The clay minerals occur mainly in the matrix. The Al-hydroxides ooids and the Al-hydroxides rims, coating the Fe-rich duricrust fragments and broken bauxite grains, may probably derive from decomposition of the clay minerals and in situ SiO_2 leaching (Bárdossy et al., 1977).

The correlation patterns of the main elements, especially for the Regia Piana deposit - the Al_2O_3/SiO_2 and the Al_2O_3/Fe_2O_3 negative correlations, the Al_2O_3/Cr_2O_3 and the Al_2O_3/TiO_2 positive correlations - show a certain degree of in situ weathering and diagenetic leaching, which should have take place after the transport and subsequent reworking of the original lateritic material. The chemical analyses show also a clear difference between the Regia Piana and all other deposits. The Regia Piana bauxite has the highest Al_2O_3 and TiO_2 values and the lowest Fe_2O_3 and Cr_2O_3 values. This could depend on the lower abundance of angular hematite-goethite fragments derived from an original Fe-duricrust, in the Regia Piana deposit. The "*bauxitophile*" elements (Cr, Ni, V, Co, and Zr) have variable contents and non-uniform distribution among the districts. The Cr distribution, as previously mentioned, could be related to Fe^{3+} distribution, having them the same geochemical properties in this environment. Ni distribution could depend on the variable initial distribution or by variable settling of materials with basic affinity on the carbonate platform. Co and V show very slight variations in the analyzed bauxite. They have two anomalous high values in two different samples: the anomalous V could be related to high concentrations of detrital trace spinel-type minerals, Co highest value probably depends on an anomalous metal enrichment associated to Fe-(hydr)oxides or clays (Künhel, 1987). Zr contents are related to zircon and baddeleyite amounts and to Zr concentrations in the Fe-Ti(hydr)oxides (Valeton, 1972). SiO_2 is slightly higher in the Regia Piana bauxite than in the other deposits, and it is also mirrored by the higher amount of kaolinite, compared with that occurring in the other deposits.

REE amounts are in general higher in the Caserta district than in the Matese Mts. deposits. We might consider that this characteristic could indicate a higher leaching of REEs experienced by the Regia Piana bauxite, than in the other deposits. Considering the positive correlation between $(La/Yb)_{ch}$ ratio and Fe_2O_3, and the association of the higher $(La/Yb)_{ch}$ values with the Fe-rich Caserta district samples, we can suppose that this behavior could be due to the scavenging characteristics of the Fe-(hydr)oxides (Künhel, 1987), which have favored a major retainment of REEs in Caserta district deposits. Moreover, Regia Piana is the only deposit which shows a LREE-HREE fractionation, with samples slightly more enriched in HREE than LREE, and samples characterized by very high $(La/Yb)_{ch}$ ratios. The fractionation and the anomalous enrichment of LREEs in the samples collected from the top of the Regia Piana profile can be related to the occurrence of authigenic LREE-minerals, as stated before. It possibly derives from the cerium oxidation process (from Ce^{3+} to Ce^{4+}) as shown for the Apulia and Nurra (Sardinia) deposits by Mongelli (1997) and Mameli et al. (2007). This enrichment can also depend on the LREE precipitation under alkaline conditions at the boundary with the hanging wall

carbonates and their adsorption on Fe-hydroxides or clay minerals, as observed by Künhel (1987) and Maksimovic and Pantó (1991).

Parental affinity of the bauxite

Most lateritic bauxites can be directly related, through their textures and composition, to the underlying source rocks (e.g., Bardossy and Aleva, 1990), but this is rarely the case for bauxites developed above carbonate sequences. Despite the well-constrained stratigraphic framework for bauxite formation, the origin of the Cretaceous karst bauxites in the Campania district, as of others in Southern Italy, remains controversial. The dissolution of the host carbonate to leave an insoluble residue is not considered a viable mechanism for bauxite formation, because the host carbonates are too pure (Bárdossy et al., 1977; D'Argenio et al., 1986; D'Argenio and Mindszenty, 1995). There is a strong possibility that bauxites in the Southern Apennines may have formed from windblown pyroclastics (D'Argenio and Mindszenty, 1995 and references therein) that covered the platform carbonates as a thin blanket, and were then subjected to lateritization and local remobilization, as in the case of the Jamaican bauxites (Comer, 1974). A ghost of a pyroxene crystal (Bàrdossy et al., 1977), the clay mineral association and geochemistry detected in the Abruzzi deposits (Morelli et al., 2000) and the Eu/Eu* and Sm/Nd data from the Apulian orebodies, which are consistent with mixing between a carbonate rock and an andesitic pyroclastite (Mongelli, 1994), are so far the only indirect evidence of a possible volcaniclastic source for the Southern Italy bauxites.

During the bauxitization process, a fractionation of major, minor and trace elements, including REE, takes place. Some ratios, especially the Eu/Eu* have proved, however, to be retained during intense weathering phenomena (Mameli et al., 2007 and references therein). In all deposits we have taken into account, the Eu/Eu* ratio shows negligible changes ($0.55 < Eu/Eu^* < 0.72$; Figure 9a).

To investigate the parental affinity of the Campania bauxites, one may consider their TiO_2/Al_2O_3 ratio. In fact, it is well known that both Al and Ti have a high potential for being transferred into the sedimentary rocks by weathering, thus preserving a record of the protoliths, since they have very low water/upper crust partition coefficients and residence times (Taylor and McLennan, 1985). In addition, Al and Ti are considered as immobile elements during bauxitization (MacLean et al., 1997) and, as a consequence, it should be possible to assume that the TiO_2/Al_2O_3 ratio is a sensitive index of parental affinity. Comparing the Eu/Eu* and TiO_2/Al_2O_3 ratios of the Campania bauxites, with several examples of upper crustal rocks (Taylor and McLennan, 1985), we see that all our samples cluster very near to the mean values of UCC (Upper Continental Crust) (Rudnick and Gao, 2003), being TiO_2/Al_2O_3 ratios around 0.05 for the bauxites and 0.03 for the UCC, and showing, on average, the same Eu/Eu* ratio (Figure 9b). These values should point to similar source materials for all deposits, which do not show a definite magmatic signature.

Another clue to the possible source of the parent material for bauxites of the Campania deposits could be also derived from the diagram of Figure 9c with their Ni and Cr contents compared with those of other Mediterranean karst bauxite ores (Kalaitzidis et al., 2010). It is possible to observe that the Campania bauxites have Ni-Cr contents very similar to those of Turkish (Öztürk et al., 2002) and Sardinian bauxites (Mameli et al., 2007), but much lower than those of Greek bauxites (Laskou and Economou-Eliopoulos, 2007). This depends on the strong "ophiolitic" signature of most Greek bauxites, which does not exist in the other deposits.

As summarized by Carannante et al. (2009), the bauxites mark a very distinctive unconformity in the Mesozoic Apennine carbonate successions.

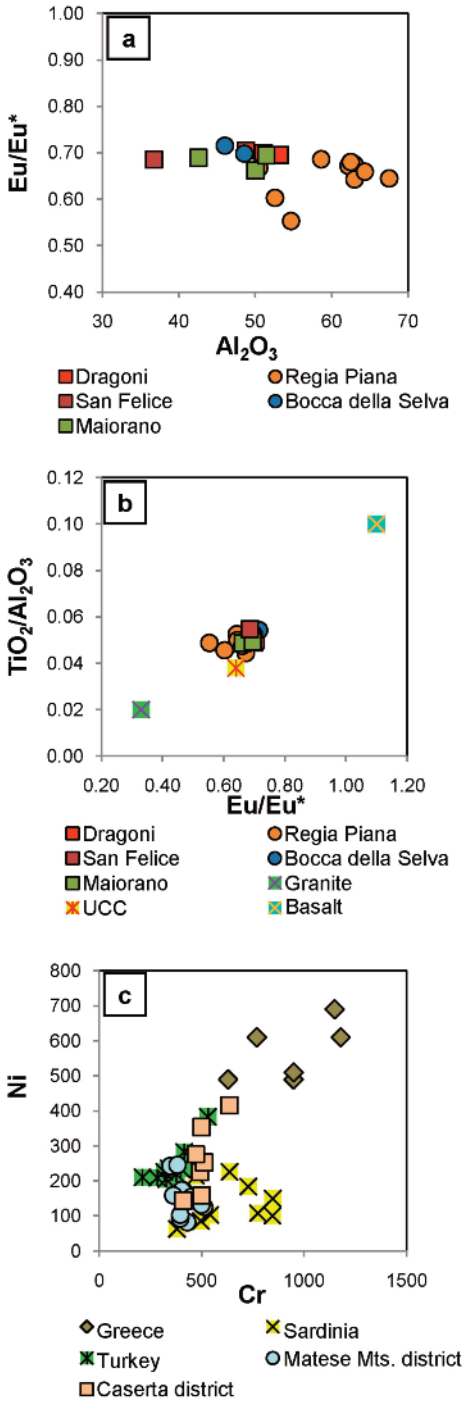

Notwithstanding, some continuous coeval successions, considered part of the same palaeogeographic domain, also exist in the same area. In these successions a greenish marls layer (Aptian) - the so-called "*livello a Orbitoline*" (De Castro, 1963), due to its prevailing micropaleontological content - occurs in place of the bauxite unconformity. Our preliminary SEM-EDS analyses on the *Orbitoline* marls from Mt. Tobenna (Salerno, Figure 1) have shown for the first time the same detrital minerals association (zircon, monazite, rutile, ilmenite, Figure 10) found in the Campania bauxites. Even if the detrital association (zircon, monazite, rutile, ilmenite) is relatively common, the similarities should suggest a possible common source material for the two sedimentary lithologies, deposited in a continental environment in the bauxite case, and in a marine environment in the "*livello a Orbitoline*" case.

Considering the Mesozoic paleogeography reported in Figure 2, and the Bahamian type character of the Apennine carbonate platform, it seems logical to reject the idea that the parental source materials for the Campania bauxite were transported on the platform through a hydrographic network and, as stated by previous authors (Bárdossy et al., 1977; D'Argenio and Mindszenty, 1995), we are inclined to agree with a windblown transport of the "would be" bauxitic material. Several detrital minerals detected in

Figure 9. a) Binary diagram between Eu/Eu* and Al_2O_3, for the analyzed deposits. b) Binary diagram between TiO_2/Al_2O_3 and Eu/Eu*, for the analyzed deposits. The values of granite, basalt and UCC (Taylor and McLennan, 1985; Rudnick and Gao, 2003), are indicated for comparison. c) Binary diagram between Ni and Cr, showing the comparison of the Matese Mts. and Caserta district bauxites with other Mediterrranean bauxites; Turkey (Öztürk et al., 2002), Sardinia (Mameli et al., 2007), Greece (Laskou and Economou-Eliopoulos, 2007). Al_2O_3 are in wt. %, Ni and Cr in ppm.

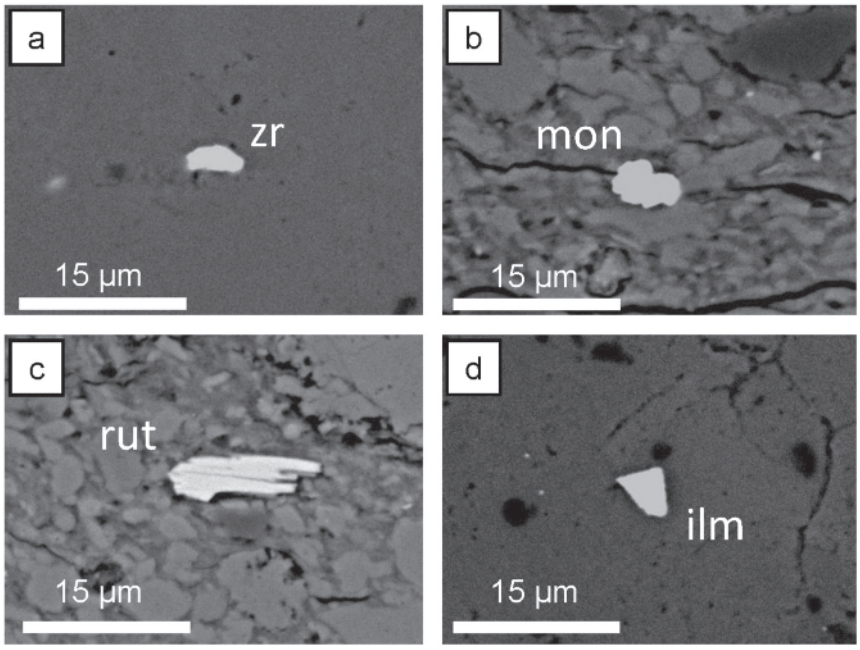

Figure 10. Backscattered electrons images (BSE) of detrital minerals in the "livello a Orbitoline", from Mt. Tobenna (Salerno, see Figure 1): a) zircon; b) monazite; c) rutile; d) ilmenite.

Southern Italy bauxites can have a "primary" volcanic origin (e.g. zircon, ilmenite, rutile, titanite), and others (e.g. monazite, qandilite spinel, quartz) can be also derived from the erosion of an ancient exposed terrain. Chemical analyses, Eu/Eu* and TiO_2/Al_2O_3 ratios and the Ni-Cr contents seem to indicate a composition of the source material more similar to the UCC than granite or basalt (Taylor and McLennan, 1995; Rudnick and Gao, 2003), even if it is not possible to clearly distinguish at this stage if the source material derives from a contemporary volcanism or from the erosion of an exposed continental terrain (or rather from both).

Conclusions

The major element and REE geochemistry shows a clear difference between the Regia Piana deposit and all the other deposits occurring in both districts. Caserta district and Bocca della Selva deposits show mean REE and iron contents higher than Regia Piana bauxite. The relationship between these chemical parameters could be due to the scavenging characteristics of the Fe-(hydr)oxides, more abundant in the Caserta district and Bocca della Selva than Regia Piana deposits. Regia Piana is the only deposit which shows a marked LREE-HREE fractionation. This is probably related to the formation of authigenic LREE-minerals in the topmost layers of the bauxite deposit.

The correlation patterns of the main elements, especially for the Regia Piana deposit show a certain degree of in situ weathering and diagenetic leaching, which should have taken place after the transport and subsequent reworking of the original lateritic material.

The analytical data gained with the present study have shed new light on the possible source of the parent material for bauxites in southern Italy. The detrital heavy mineral association detected (SEM-EDS and QEMSCAN®) in all deposits may suggest not only a windblown volcanic source material for the bauxites (Dinarides explosive volcanism?), as hypothesized in literature (Bárdossy et al., 1977), but also a partial origin from an exposed terrain. The exact nature and paleogeographic position of this source could not be determined, however, by chemical analyses of major and trace elements (including REE), Eu/Eu* and TiO_2/Al_2O_3 ratios and Ni-Cr contents. A similar detrital association has also been found in the Aptian "*Orbitoline*" marls, which are marine sediments supposed to be the non-weathered equivalent of bauxites. Due to the isolated position of the Appennine carbonate platform during Cretaceous, the paleogeographic model precludes any possible fluviomarine transport for the source material of the bauxites.

The preliminary QEMSCAN® analysis allowed rapid quantification of mineralogy (including the trace detrital phases) and assessment of the individual textural characteristics of the bauxite lithotypes, showing a detailed image of the distribution of economic and non-economic minerals and their intergrowths. Further development work with QEMSCAN® is required to refine the mineral database identifications for the Campania bauxite ores, considered as a model analogue for truly economic karst bauxite deposits.

Acknowledgements

This study has been carried out with research funds of University of Napoli granted to M. Boni. R. de Gennaro (CISAG, Napoli) is thanked for technical assistance during SEM-EDS analyses. Thanks are due to G.G. Acerbo, R. Buccione and R. Aiello for help during the field and analytical works.

A special thank is also due to the reviewers, who have helped to improve a first version of this paper.

References

Bárdossy G. (1982) - Karst bauxites, bauxite deposits on carbonate rocks. *Developments in Economic Geology,* 14, Amsterdam, Elsevier, 441 pp.

Bárdossy G. and Aleva G.J.J. (1990) - Lateritic bauxites. Amsterdam, Elsevier, 624 pp.

Bárdossy G., Boni M., Dall'Aglio M., D'Argenio B., Pantò G. (1977) - Bauxites of peninsular Italy. Composition, origin and geotectonic significance. (Gebr. Borntraeger). *Monographic series on Mineral Deposits*, 15, 1-61.

Bonardi G., D'Argenio B. and Perrone V. (1988) - Carta geologica dell'Appennino meridionale alla scala 1:250.000. *Memorie della Società Geologica,* 41.

Carannante G., D'Argenio B., Ferreri V. and Simone L. (1987) - Cretaceous paleokarst of the Campanian Appennines from early diagenetic to late filling stage. A case history. *Rendiconti Società Geologica Italiana*, 9, 251-256.

Carannante G., D'Argenio B., Mindszenty A., Ruberti D. and Simone L. (1994) - Cretaceous-Miocene shallow water carbonate sequences. Regional unconformities and facies patterns. 15th IAS Regional Meeting, April 1994, Ischia, Italy, Field Trip Guidebook, 27-60.

Carannante G., Pugliese A., Ruberti D., Simone L., Vigliotti M. and Vigorito M. (2009) - Evoluzione Cretacica di un settore della piattaforma apula da dati di sottosuolo e di affioramento (Appennino campano-molisano). *Bollettino delle Societá Geologica Italiana*, 128, 3-31.

Carmignani L., Decandia F.A., Disperati L., Fantozzi P.L., Kligfiled R., Lazzarotto A., Liotta D. and Meccheri M. (2001) - Inner Northern Apennines. In Vai, G.B., and Martini, I.P. eds., Anatomy of an Orogen: The Apennines and Adjacent Mediterranean Basins. Kluwer Academic Publishing, Great Britain, 197-214.

Channell J.E.T., D'Argenio B. and Hovarth F. (1979) - Adria, the African promontory, in Mesozoic Mediterranean paleogeography. *Earth Sciences Reviews*, 15, 213-292.

Comer J.B. (1974) - Genesis of Jamaican bauxite. *Economic Geology*, 69, 1251-1264.

Crescenti U. and Vighi L. (1970) - Risultati delle ricerche eseguite sulle formazioni bauxitiche cretaciche del Casertano e del Matese in Campania. *Memorie della Società Geologica Italiana*. 9, 401-

434.

D'Argenio B. and Mindszenty A. (1995) - Bauxites and related paleokarst: Tectonic and climatic event markers at regional unconformities. *Eclogae Geologicae Helvetiae,* 88, 453-499.

D'Argenio B., Mindszenty A., Bárdossy G., Juhász E., Boni M. (1986) - Bauxites of southern Italy revisited. *Rendiconti della Società Geologica Italiana*, 9, 263-268.

D'Argenio B., Pescatore T. and Scandone P. (1973) - Schema geologico dell'Appennino meridionale. *Atti dell'Accademia Nazionale dei Lincei*, 183, 49-72.

De Castro P. (1963) - Nuove osservazioni sul livello ad Orbitoline in Campania. *Bollettino della Società dei Naturalisti, Napoli*, 71, 103-135.

Dercourt J., Ricou L.E. and Vrielynck B. (1993) - Atlas Tethys Palaeoenvironmental Maps. P. Gauthier-Villars, Paris, p. 307, 14 maps.

Dewey J.F., Helman M.L., Turco E., Hutton D.H.W. and Knott S.D. (1989) - Kinematics of the western Mediterranean. In: Coward, D., Dietrich, D., and Park, R.G. eds., Alpine Tectonics: Geological Society of London Special Publication, 45, 265-283.

Goodall W.R. and Scales P.J. (2007) - An overview of the advantages and disadvantages of the determination of gold mineralogy by automated mineralogy. *Minerals Engineering*, 20, 506-517.

Gottlieb P., Wilkie G., Sutherland D., Ho-Tun E., Suthers S., Perera K., Jenkins B., Spencer S., Butcher A. and Rayner J. (2000) - Using quantitative electron microscopy for process mineralogy applications. *Journal of the Minerals, Metals and Materials Society,* 52, 24-27.

Kalaitzidis S., Siavalas G., Skarpelis N., Araujo C.V. and Christanis K. (2010) - Late Cretaceous coal overlying karstic bauxite deposits in the Parnassus-Ghiona Unit, Central Greece: coal characteristics and depositional environment. *International Journal of Coal Geology,* 81-4, 211-226.

Künhel R.A. (1987) - The role of cationic and anionic scavengers in laterites. *Chemical Geology*, 60, 31-40.

Laskou M. and Economou-Eliopoulos M. (2007) - The role of microorganisms on the mineralogical and geochemical characteristics of the Parnassos-Ghiona bauxite deposits, Greece. *Journal of Geochemical Exploration,* 93, 67-77.

MacLean W.H., Bonavia F.F. and Sanna G. (1997) - Argillite debris converted to bauxite during karst weathering: evidence from immobile element geochemistry at the Olmedo Deposit, Sardinia. *Mineralium Deposita*, 32, 607-616.

Maksimovic Z.J. and Pantó G. (1991) - Contribution to the geochemistry of the rare earth elements in the karst-bauxites deposits of Yugoslavia and Greece. *Geoderma*, 51, 93-109.

Maliverno A. and Ryan W.B. (1986) - Extension in the Tyrrhenian Sea and shortening in the Apennines as a result of arc migration driven by sinking of the lithosphere. *Tectonics,* 5, 227-246.

Mameli P., Mongelli G., Oggiano G. and Dinelli E. (2007) - Geological, geochemical and mineralogical features of some bauxite deposits from Nurra (Western Sardinia, Italy): insight on conditions of formation and parental affinity. *International Jounal of Earth Science*, 96, 887-902.

Mazzoli S. and Helman M. (1994) - Neogene patterns of relative plate motion for Africa- Europe: some implications for recent Central Mediterranean tectonics. *Geologische Rundschau*, 83, 464- 468.

Mazzoli S., D'Errico M., Aldegna L., Corrado S., Invernizzi C., Shiner P. and Zattin M. (2008) - Tectonic burial and "young" (< 10 Ma) exhumation in the southern Apennines fold-and-thrust belt (Italy). *Geology*, 36, 243-246.

Mongelli G. (1994) - Le bauxiti carsiche apule: composizione chimica e modello genetico. *Plinius*, 12, 72-74.

Mongelli G. (1997) - Ce-anomalies in the textural components of Upper Cretaceous karst bauxites from the Apulian carbonate platform (Southern Italy). *Chemical Geology*, 140, 69-79.

Morelli F., Cullers R., Laviano R. and Mongelli G. (2000) - Geochemistry and palaeoenvironmental significance of Upper Cretaceous clay-rich beds from the Peri-adriatic Apulia carbonate platform, southern Italy. *Periodico di Mineralogia*, 69, 165-183.

Özrtürk H., Hein J.R. and Hanilci N. (2002) - Genesis of the Dogankuzu and Mortas Bauxite Deposits, Taurides, Turkey: Separation of Al, Fe, and Mn and Implication for Passive Margin Metallogeny. *Economic Geology*, 97, 1063-1077.

Parotto M. and Praturlon A. (1975) - Geological summary of Central Apennines. *Quaderni de "La ricerca scientifica", Consiglio Nazionale delle Ricerche*, 90, 257-311.

Patacca E. and Scandone P. (2007) - Geology of the

Southern Apennines. *Bollettino della Società Geologica Italiana*, Special Issue 7, 75-119.

Pirrie D., Butcher A.R., Power M.R., Gottlieb P. and Miller G.L. (2004) - Rapid quantitative mineral and phase analysis using automated scanning electron microscopy (QEMSCAN®); potential applications in forensic geoscience. In: Pye K., Croft D.J. (Eds.), Forensic Geoscience, Principles, Techniques and Applications, 232, Geological Society Special Publication, London, 123-136.

Rollinson,G., Andersen J.C.Ø., Stickland R.J., Boni M. and Fairhurst R. (2011) - Characterisation of non-sulphide zinc deposits using QEMSCAN. *Minerals Engineering*, 24, 778-787.

Royden L., Patacca E. and Scandone P. (1987) - Segmentation and configuration of subducted lithosphere in Italy: an important control on thrust-belt and foredeep-basin evolution. *Geology*, 15, 714-717.

Rudnick R.L. and Gao S. (2003) - Composition of the continental crust. In: Rudnick R.L.(Ed.), The crust: Treatise in Geochemistry, Vol. 3, Amsterdam, Elsevier, 1-64.

Scandone P. (1972) - Studi di geologia lucana: carta dei terreni della serie calcareo-silico-marnosa e note illustrative. *Bollettino della Società dei Naturalisti in Napoli*, 81, 225-300.

Schettino A. and Turco E. (2011) - Tectonic history of the western Tethys since the Late Triassic. *Geological Society of America Bulletin*, 123, 89-105.

Taylor S.R. and McLennan S.M. (1985) - The continental crust: its composition and evolution. *Blackwell, Oxford*, pp. 1-312.

Taylor S.R. and McLennan S.M. (1995) - The geochemical evolution of the continental crust. *Reviews of Geophysics*, 33, 241-265.

Valeton I. (1972) - Bauxites. *Developments in Soil Science,* 1, Amsterdam, Elsevier, 226 pp.

Submitted, July 2011 - Accepted, November 2011